frontiers | Frontiers in Marine Science

TYPE Original Research
PUBLISHED 05 February 2025
DOI 10.3389/fmars.2025.1524885

OPEN ACCESS

EDITED BY
Marialetizia Palomba,
University of Tuscia, Italy

REVIEWED BY
Antonio Calisi,
Università del Piemonte Orientale, Italy
Maria Luisa Vannuccini,
University of Tuscia, Italy

*CORRESPONDENCE
Min Pang
pm_cat@hotmail.com
Pei Jiang
jiangpeicsu@sina.com
Pei Qu
qupei@fio.org.cn

†These authors have contributed equally to this work and share first authorship

RECEIVED 08 November 2024
ACCEPTED 20 January 2025
PUBLISHED 05 February 2025

CITATION
Yu Q-Q, Zhang Y, Zhao S, Pang M, Jiang P and Qu P (2025) Comprehensive analysis of ionomic profiling in *Chlorella* exposed to chlorpyrifos. *Front. Mar. Sci.* 12:1524885. doi: 10.3389/fmars.2025.1524885

Comprehensive analysis of ionomic profiling in *Chlorella* exposed to chlorpyrifos

Qing-Qing Yu[1†], Yulong Zhang[2†], Shiyuan Zhao[1], Min Pang[2*], Pei Jiang[1*] and Pei Qu[2*]

[1]Translational Pharmaceutical Laboratory, Jining NO.1 People's Hospital, Jining, China, [2]Marine Ecology Research Center, First Institute of Oceanography, Ministry of Natural Resources of the People's Republic of China, Laoshan District, Qingdao, China

Introduction: Chlorpyrifos (CPF), a widely used organophosphorus insecticide, is highly toxic to non-target aquatic organisms and has relatively high persistence in water, posing a serious threat to marine ecosystems. However, little is known about the toxicological mechanism of CPF on marine microalgae, which is the main primary producer in the marine ecosystem.

Methods: This study explored the ion changes of microalgae *Chlorella vulgaris* under the stress of CPF through Inductively Coupled Plasma Mass Spectrometry (ICP-MS).

Results: Significant disparities in ionomics among control and treatment group were observed through pattern recognition analysis (principal component analysis, PCA; orthogonal partial least squares discriminant analysis, OPLS-DA), indicating that CPF may impede their growth by disrupting the homeostasis of crucial elements within algal cells.

Discussion: This study elucidated the inhibitory impact of CPF on green algae growth and its potential mechanism of toxicity through ICP-MS, providing crucial insights for a comprehensive understanding of the influence of organophosphorus pesticides on aquatic ecosystems.

KEYWORDS

chlorpyrifos, ionomics, ICP-MS, microalgae, organophosphorus insecticide

1 Introduction

Chlorpyrifos (CPF), a highly effective and broad-spectrum organophosphorus insecticide with contact, stomach poison and fumigation effects, is widely used globally to control crop damage from various insects, including borers, scale insects, armyworms, aphids and mites (Li et al., 2021). The insecticidal effect of CPF primarily involves the inhibition of acetylcholinesterase (AChE) (Ubaid ur Rahman et al., 2021). This inhibition results in the overstimulation of neuronal cells and disorders of central nervous system. In severe cases, it can lead torespiratory failure, paralysis, and even death (Ubaid ur Rahman et al., 2021).

Excessive utilization and misuse of CPF inevitably impacts the ecological environment (Li et al., 2021). When applied on farmland, CPF has an actual biological uptake rate of less than 1% (Bellas et al., 2023), with the majority being lost during field application. During its migration, CPF poses potential toxic effects on non-target organisms and even humans. Studies have demonstrated that CPF degrades soil fertility by inhibiting nitrogen and phosphorus metabolism, disrupting the acid-base balance, and contaminating groundwater (Nandi et al., 2022). In addition, CPF adversely affects non-target soil organisms such as earthworms, with LC_{50} values ranging from 118.5 to 148 mg/kg (Zhou et al., 2008), leading to a decreases in soil biodiversity and consequently negatively impacting agroecosystems.

Acute intoxication from short-term exposure to high doses of CPF can lead to symptoms including dizziness, headache, convulsions, increased sweating, salivation, nausea, unconsciousness, and even death (Nandi et al., 2022). Even at the does below the threshold for systemic toxicity, prolonged CPF exposure over months or years may result in chronic effects such as impaired neural cell development, birth defects, reproductive abnormalities, and an increased risk of cancer (Nandi et al., 2022).

CPF has been detected in freshwater worldwide due to its misuse, particularly in the water sources near the application area (Affum et al., 2018; Kar et al., 2024). The CPF content in Ankobra Basin (Ghana) groundwater ranged from30 to 2000ng/L (Affum et al., 2018), while those in stream near Paddyfields in Odisha, India)were 81.53 ng/L on average (Kar et al., 2024). Given its high toxicity to non-target aquatic organisms and relatively long persistence in water, CPF poses a significant threat to aquaponic systems (Bellas et al., 2023). Studies have shown that CPF can inhibit the growth of various freshwater microalgae, such as *Scenedesmus quadricanda*, with a 96 h EC_{50} value of 708.01 μg/L (Sun et al., 2013). Toxicity of CPF to aquatic fauna includes disruption in steroid metabolism, hepatic system dysfunction, behavioral changes, epithelial hyperplasia, respiratory stress, hydropic degeneration, delayed metamorphosis, renal tubule degeneration and necrosis, and glomerular shrinkage (Nandi et al., 2022). At a concentration of 0.0528 μg/L, CPF caused mortality in Daphnia. The 90-hour LC_{50} values for CPF in carp, crucian carp and silver carp were 3 170, 3 670 and 3 970 μg/L, respectively (Zhao et al., 2008).

The ocean has long been considered the ultimate sink for pesticides (Bellas et al., 2023). Due to the misuse of CPF, CPF can be detected in coastal and even polar marine areas worldwide (Zhong et al., 2012; Smalling et al., 2013; Montuori et al., 2015; Liu et al., 2018). According to the reported toxicological studies, CPF is toxic to many marine species. Microalgae, the main primary producer in the marine ecosystem, are not likely to be very sensitive to CPF because it does not have the processes, structures, or functional groups involved in the modes of action of CPF. The growth of the marine diatoms *Skeletonema costatum* and *Minutocellus polymorus* were affected by CPF at 640 and 240 μg/L, respectively (Walsh et al., 1988). Crustaceans, as "Marine insects", have similar biochemical and physiological traits with target organisms, therefore it is especially sensitive to CPF. *Palaemonetes pugio* showed LC50 values of 0.37 μg/L (Key and Fulton, 1993), *Neomysis integer* showed LC50 values of 0.13μg/L (Roast et al., 1999). In general, Crustaceans is more sensitive to CPF than marine fish. Species and life-stage of marine fish depended its sensitivity to CPF, adults have been found to be more tolerated to CPF than juveniles and larvae. Acute lethal toxicity of CPF to *Menidia peninsulae* larvae and Cyprinodon variegatus has been reported at 0.42 and 270 μg/L (EPA, 1986), respectively.

To safeguard human health, ecological safety, and ensure food security globally, various countries, including China, have comprehensively banned the use of CPF (Huang et al., 2020). Nevertheless, CPF remains the most extensively employed organophosphorus insecticide worldwide (Jiang et al., 2021).The CPF levels now in the ocean has been found in small amounts (8~219.42 pg/L, Supplementary Table S1) after undergoing processes such as dilution, photolysis, biodegradation, and adsorption settling in seawater, which are too low to cause significant acute toxic effects on marine organisms (Bellas et al., 2023). However, studies have shown that long-term exposure to low concentrations can result in CPF accumulation in various tissues of tilapia fish, leading to chronic toxicity effects over time (Rao et al., 2003). CPF has also been detected in different groups of marine organisms worldwide, confirming its ability to accumulate within these organisms (Supplementary Table S2) (Solé et al., 2000; Smalling et al., 2013; Ros et al., 2015; Balmer et al., 2019). Given that global marine fisheries production has reached 91.03 million tons in 2022 (FAO, 2024), humans who rely on marine organisms as a source of high-quality protein are also at risk of exposure to CPF. Therefore, it is necessary to improve the knowledge of the mechanism of CPF toxicity on aquatic organisms. Microalgae are main primary producer in the marine ecosystems. They face, absorb, and accumulate CPF from seawater directly (Morris et al., 2016), but little has been done on the toxicological mechanism of CPF on marine microalgae.

Ionome includes all the mineral nutrients and trace elements existing in an organism and represents the inorganic component of cellular system, which are involved in a wide range of crucial biological processes, such as signaling, osmoregulation, enzymology, electrophysiology and transport (Singh et al., 2022). Ion changes in a process means large changes has happened to related metabolic pathways. Thus, ionomics, dealing with the changes in ion production, provides a new perspective to the study toxicological mechanisms of microalgae under varied external stimulus (Zargar et al., 2016). This study aims to investigate the impact of CPF on the biological behavior of microalgae *Chlorella vulgaris*, and to explore the toxicological mechanisms of CPF on *C. vulgaris* using ionomics. This study aims to provide novel insights into pollution research, focusing on the effects of bioaccumulation and biomagnification, their impacts along the trophic chains and the consequent alteration of marine ecosystems.

2 Methods

2.1 Chemicals and reagents

Chlorpyrifos (Figure 1) (powder, 99.61% purity, CAS#: 2921-88-2) was obtained from Dr. Ehrenstorfer Co., Ltd (Augsburg, Germany). For the experiments, stock solutions of CPF was prepared in dimethyl sulfoxide (DMSO) and diluted into the

10.3389/fmars.2025.1524885

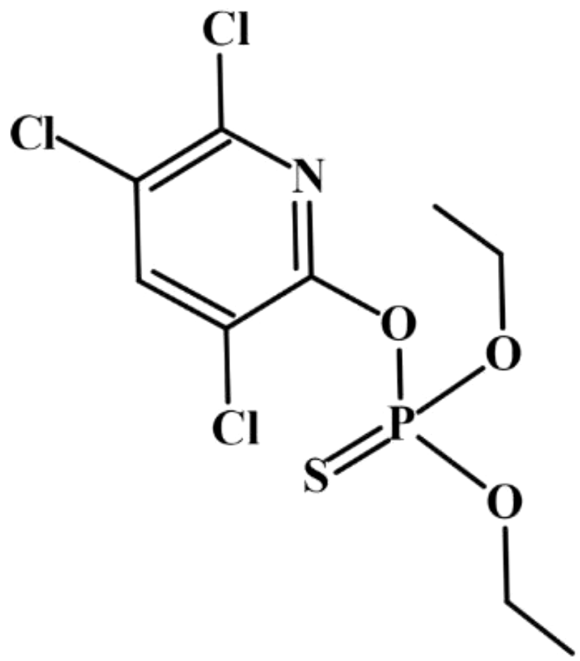

FIGURE 1
Chlorpyrifos, IUPAC name is *O, O*-Diethyl-*O*-(3,5,6-trichloro-2-pyridyl) phosphorothioate, is a white crystal-like solid with a strong odor. It does not mix well with water, so it is usually mixed with oily liquids before it is applied to crops or animals.

culture media to the desired concentrations. In the culture media the final concentration of DMSO was < 0.1%. F/2 medium (Guillard, 1975), and Lugo's iodine solution were used.

2.2 Culture condition

The First Institute of Oceanography (MNR, Qingdao, China) provided cultures of the unicellular microalga *Chlorella vulgaris*. The strains were used to prepare the stock culture. To obtain a culture in the early exponential growth phase, it was incubated for 3 days at a temperature of 23 ± 1°C under fluorescent illumination of 4000 lx and a light/dark cycle of 12/12 hours in an illumination incubator. Manual swirling agitations were performed three times daily. The microalga strain was inoculated at a concentration of 25% ($V_{inoculum}/V_{media}$) in 150 mL sterile f/2 medium contained in glass Erlenmeyer flasks with a volume capacity of 250 mL. The culture medium was supplemented with CPF stock solutions to achieve nominal concentrations of the active ingredient: 0, 50, 100, 150, and 200 µg/L. A control treatment without any DMSO was also included in the same sterile f/2 medium. All experiments were conducted in triplicate without replacing the medium throughout the study period. To ensure uniform light and temperature conditions, all flasks containing different treatments were repositioned three times daily inside the illumination incubator during the course of the experiment. To assess the impacts of chlorpyrifos on the population growth, the density of *Chlorella* in each treatment was figured by direct counting in Neubauer chamber every 24 h during the entire experimental period (12 days).

2.3 Sample collection and preparation

At the end of the bioassay, the DMSO control culture and the treatment groups exposed to CPF concentrations of 0, 50, 100, 150, 200 µg/L were centrifuged at 4000 rpm for 10 min. The resulting pellet was refrigerated at -20 °C for subsequent ICP-MS analysis. The CPF concentrations in the experimental groups were determined based on previous studies and preliminary experiments conducted for this study.

2.4 ICP-MS

Prior to the experiment, all experimental materials were soaked in 6M nitric acid overnight, followed by rinsing and drying with ultrapure water before use. A digestion tube was utilized to hold 50 µL of serum or 50 mg of tissue, which was then supplemented with 1ml of 65% nitric acid. The mixture underwent digestion on a heating plate at a temperature of 130 °C for a duration of two hours. After evaporating the acid, it was diluted using ultrapure water. Before injection, the sample was cooled down to room temperature. In this study, detection was conducted using the NexION 1000G ICP-MS spectrometer (PerkinElmer, USA), which underwent tuning optimization through mass spectrometry tuning solution prior to analysis initiation. Calibration involved online internal standard addition and collision mode employed high-purity helium gas as the collision gas for interference removal purposes. The instrument's operating parameters were set as follows: nebulizer flow rate at 1.04 L/min, auxiliary gas flow rate at 1.20 L/min, plasma gas flow rate at15 L/min, ICP RF power at1600 W, simulated voltage -1862 V, pulse voltage at1250 V, and blank removal process applied. The chamber was supplied with an internal standard solution, which consisted of scandium, germanium, indium, and rhenium at a concentration of 20 µg/L. This solution was introduced into the chamber using a peristaltic pump. A total of 34 elements were identified in the analysis, including lithium (Li), beryllium (Be), boron (B), sodium (Na), magnesium (Mg), aluminum (Al), silicon (Si), phosphorus (P), potassium (K), calcium(Ga), titanium (Ti), vanadium (V), chromium (Cr), manganese (Mn), iron (Fe), cobalt (Co), nickel (Ni), copper (Cu), zinc (Zn), arsenic (As), selenium (Se), strontium (Sr), zirconium (Zr), molybdenum (Mo), silver (Ag), cadmium (Cd), tin(Sn), antimony (Sb), barium (Ba), thallium (Tl), lead (Pb), bismuth (Bi), mercury (Hg). After excluding elements that deviated from the standard curve or had concentrations below the limit of quantification, a total of 28 elements remained: Li, Na, Mg, Al, P, K, Ca, Ti, V, Cr, Mn, Fe, Co, Ni, Cu, Zn, As, Se, Sr, Zr, Mo, Ag, Cd, Sn, Sb, Ba, Ir, Pb, Bi. The accuracy, reproducibility, and limit of quantification for this method were calculated and validated.

2.5 Multivariate statistical analysis

The data was normalized and subjected to pattern recognition analysis using SIMCA-P 14.0 (Umetrics, Umeå, Sweden),

employing principal component analysis (PCA) and orthogonal partial least squares discriminant analysis (OPLS-DA). Data analysis involved a two-tailed Student's t-test. The selection of differential variables was based on the following criteria: (1) $p < 0.05$ and (2) Variable Importance in Projection (VIP) value obtained from OPLS-DA > 1.

3 Results

3.1 Establishment of *Chlorella* model treated by CFP

We counted the cells regularly every day during the culture period, and the density changes of *Chlorella* were recorded (Figure 2). Fisher-test was used to compare the mean value of *Chlorella* concentration data among the groups (Figure 3).

The *Chlorella* density map showed that the cell density of each group had an overall increasing trend, and the density of DMSO control group and 0 μg/L group was higher than that of CPF addition group, indicating that CPF had an effect on *Chlorella* growth (Figure 2). The result of Fisher-test showed that there were significant difference between 200 μg/L group and 0 μg/L group ($p < 0.05$), and nonsignificant differences between other groups, which means that 200 μg/L CPF could significantly inhibit the growth of *Chlorella* population.

3.2 Quality control of ionomics

The Correlation coefficient for the standard samples was calculated, all of which exhibited values above 0.99. The element Cd was excluded due to a Trueness/Recovery rate of 71%. Additionally, Be, As, Se, Mo, Cd, Sb, Ti and Bi were eliminated as they had fewer than one instance of detection below the Limit of quantification. The remaining elements that could be assessed include Li, B, Na, Mg, Al, P, K, Ca, Ti, V, Cr, Mn, Fe, Co, Ni, Cu, Zn, Sr, Zr, Sn, Ba, and Pb. All indicators of QC are shown in Table 1.

3.3 General linear model of ionomics

To better assess inter-group ion differences, we initially employed a linear model to evaluate disparities between the Control group and CPF groups. The results, presented in Table 2, revealed statistically significant variations in ionomics across the five groups. However, no statistically significant distinctions were observed when comparing Control with DMSO (Supplementary Table S3). Subsequent pairwise comparisons between the Control and CPF groups unveiled notable discrepancies in Li, P, Ca, Ti, and Mn (Table 3).

3.4 PCA of ionomics

We initially conducted a principal component analysis (PCA) using the data from the Control group and different doses of CPF treatment groups. The PCA model identified 2 principal components (Figure 4A) with main parameters: R2X=0.734, Q2 = 0.615. No significant outliers were observed in DModX (Figures 4B-D), indicating that the included indicator data was stable and free from anomalies. However, this PCA model did not effectively classify the data from each group (Supplementary Figure S1). Therefore, we will proceed to perform orthogonal partial least squares discriminant analysis (OPLS-DA) between Control group and different doses of CPF treatment groups.

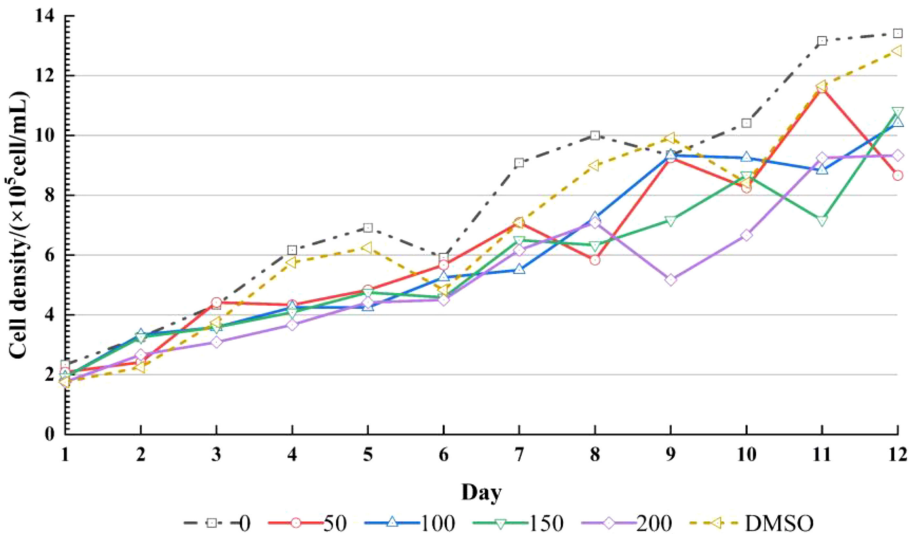

FIGURE 2
Growth of alga among DMSO Control, 0 μg/L, 50 μg/L, 100 μg/L, 150 μg/L, 200 μg/L (n=3).

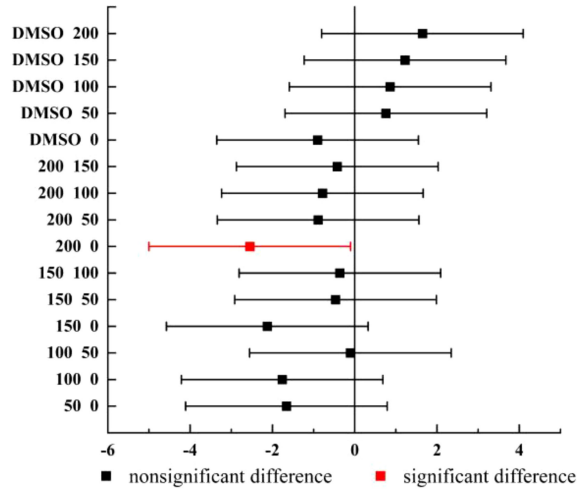

FIGURE 3
Fisher-test results between the cell density of groups (n=3).

3.5 OPLS-DA of ionomics

General linear model of ionomics showed that statistically significant variations in ionomics across the five groups. Further PCA model of ionomics revealed that no significant outliers in the data from the Control group and different doses of CPF treatment groups. But this PCA model did not effectively classify the data from each group, we then established OPLS-DA model of ionomics of Control *vs*. CPF 50 μg/L, Control *vs*. CPF 100 μg/L, Control *vs*. CPF 150 μg/L, and Control *vs*. CPF 200 μg/L, which parameters approaching 1.0 indicate that the models were stable and predictably reliable. And the significantly different element (OPLS-DA: VIP > 1 and Student's t-test: $p < 0.05$) was Mn, P, Zn, and K in Control *vs*. CPF 50 μg/L; Zn, Mn, and P in Control *vs*. CPF 100 μg/L; Ti and Ca in Control *vs*. CPF 150 μg/L; Ti, Li and Ca in Control *vs*. CPF 200 μg/L.

3.5.1 Control *vs*. CPF 50 μg/L

The OPLS-DA model of ionomics between Control and CPF 50 μg/L identified 1 + 4 principal components (Figure 5A) with main parameters: R2X=0.924, R2Y=0.92, Q2 = 0.726. Figure 5B showed this model classified the data of two groups well. Statistical validation using OPLS-DA demonstrated no signs of overfitting, as indicated by the blue regression line intersecting the vertical axis on the left side below zero. Furthermore, all Q2-values on the left were found to be lower than the original points (Figure 5C). The parameters approaching a value of 1.0 suggest that this model exhibited stability and reliable predictability. Then we calculated the VIP predictive value of each element with significant changes based on the Student's *t*-test ($p < 0.05$) and VIP score (VIP > 1, Supplementary Table S4) screening between Control and CPF 50 μg/L (Figure 5D). As Figure 6 showed, the significantly different element was Mn, P, Zn, and K.

3.5.2 Control *vs*. CPF 100 μg/L

The OPLS-DA model of ionomics between Control and CPF 100 μg/L identified 1 + 2 principal components (Figure 7A) with main parameters: R2X=0.843, R2Y=0.829, Q2 = 0.502. Figure 7B showed this model also classified the data of two groups well. Similarly to the OPLS-DA model of ionomics between Control and CPF 50 μg/L, statistical validation using OPLS-DA model of ionomics between Control and CPF 100 μg/L revealed no overfitting; all Q2-values on the left were lower than the original

TABLE 1 Quality control of ionomics.

Element	Correlation coefficient (r)	Limit of quantification	Repeatability CV	Trueness/Recovery
Li	0.999995	0.052	0.019	96.05%
B	0.999272	2.720	0.128	99.51%
Na	0.993609	91.013	0.092	198.33%
Mg	0.999765	0.601	0.019	101.81%
Al	0.999768	0.980	0.024	100.35%
P	0.999728	6.886	0.037	106.88%
K	0.999773	5.315	0.087	100.67%
Ca	0.993403	6.664	0.058	107.76%
Ti	0.999980	0.065	0.017	92.92%
V	0.999998	0.012	0.017	92.12%
Cr	0.999974	0.065	0.016	91.26%
Mn	0.999830	0.023	0.015	100.63%
Fe	0.999478	0.652	0.027	102.73%

(Continued)

TABLE 1 Continued

Element	Correlation coefficient (r)	Limit of quantification	Repeatability CV	Trueness/Recovery
Co	0.999995	0.004	0.014	91.75%
Ni	0.999968	0.099	0.017	90.35%
Cu	0.999882	0.075	0.015	87.58%
Zn	0.999826	0.456	0.015	101.36%
As	0.999957	0.396	0.017	93.79%
Se	0.999421	0.487	0.029	98.77%
Sr	0.999999	0.033	0.018	89.30%
Zr	0.999961	0.111	0.019	91.71%
Mo	0.999924	0.237	0.018	92.70%
Ag	0.998516	1.959	0.020	71.15%
Cd	0.999779	0.158	0.015	89.59%
Sn	0.998383	0.183	0.018	84.05%
Sb	0.995511	0.110	0.016	85.79%
Ba	0.999995	0.028	0.015	87.32%
Tl	0.999871	0.012	0.016	92.66%
Pb	0.999952	0.015	0.016	92.48%
Bi	0.999833	0.044	0.016	89.98%

The relevant parameters of the ions that meet the quality control criteria outlined in the research design include: correlation coefficient (r), limit of quantification (LOQ), repeatability coefficient of variation (CV), trueness/recovery rate, with n=6 for each parameter.

points (Figure 7C). The parameters approaching 1.0 indicate that this model was stable and predictably reliable. Then the VIP predictive value of each element with significant changes based on the Student' s *t*-test ($p < 0.05$) and VIP score (VIP > 1, Supplementary Table S5) screening between Control and CPF 100 µg/L (Figure 7D). As Figure 8 showed, the significantly different element was Zn, Mn, and P.

3.5.3 Control *vs.* CPF 150 µg/L

The OPLS-DA model of ionomics between Control and CPF 150 µg/L identified 1 + 1 principal components (Figure 9A) with main parameters: R2X = 0.76, R2Y = 0.713, Q2 = 0.541. Figure 9B showed this model also classified the data of two groups well. And statistical validation using OPLS-DA model of ionomics between Control and CPF 150 µg/L revealed no overfitting; all Q2-values on the left were lower than the original points (Figure 9C). Then the VIP predictive value of each element with significant changes based on the Student's *t*-test ($p < 0.05$) and VIP score (VIP > 1, Supplementary Table S6) screening between Control and CPF 150 µg/L (Figure 9D). As Figure 10 showed, the significantly different element was Ti and Ca.

TABLE 2 General linear model analysis of ionomic profile across Control, CPF 50 µg/L, CPF 100 µg/L, CPF 150 µg/L, and CPF 200 µg/L groups.

	Statistic	F	*p*-value
Wilks' lambda	3.594	2.815	0.001*
Pillai's trace	0.000	3.740	0.001*
Lawley-Hotelling trace	165.588	4.704	0.005*
Roy's largest root	132.069	42.022	0.000**

(* indicates $p<0.05$, while ** indicates $p<0.01$; n=6).

3.5.4 Control *vs.* CPF 200 µg/L

The OPLS-DA model of ionomics between Control and CPF 200 µg/L identified 1 + 1 principal components (Figure 11A) with main parameters: R2X = 0.759, R2Y = 0.792, Q2 = 0.559. Figure 11B showed this model also classified the data of two groups well. And statistical validation using OPLS-DA model of ionomics between Control and CPF 200 µg/L revealed no overfitting; all Q2-values on the left were lower than the original points (Figure 11C). Then the VIP predictive value of each element with significant changes based on the Student's *t*-test ($p < 0.05$) and VIP score (VIP > 1, Supplementary Table S7) screening between Control and CPF 200 µg/L (Figure 11D). As Figure 12 showed, the significantly different element was Ti, Li and Ca.

4 Discussion

Microalgae exhibit higher tolerance to the toxic effects of CPF due to the absence of processes, structures, or functional groups

10.3389/fmars.2025.1524885

TABLE 3 The pairwise comparisons between Control and CPF 50 μg/L, CPF 100 μg/L, CPF 150 μg/L, and CPF 200 μg/L.

Element	Group		Average-variance	*p*-value	95%CI	
					Lower	Upper
Li	Control	CPF 50 μg/L	0.004	0.971	-0.201	0.209
		CPF 100 μg/L	-0.007	0.948	-0.212	0.199
		CPF 150 μg/L	-0.236	0.026*	-0.441	-0.031
		CPF 200 μg/L	-0.075	0.458	-0.280	0.130
P	Control	CPF 50 μg/L	1054.407	0.040*	51.877	2056.937
		CPF 100 μg/L	983.920	0.054	-18.610	1986.450
		CPF 150 μg/L	126.757	0.797	-875.773	1129.287
		CPF 200 μg/L	-13.235	0.979	-1015.765	989.294
Ca	Control	CPF 50 μg/L	81.074	0.519	-174.054	336.202
		CPF 100 μg/L	96.601	0.443	-158.527	351.729
		CPF 150 μg/L	-317.652	0.017*	-572.780	-62.525
		CPF 200 μg/L	-288.736	0.028*	-543.864	-33.608
Ti	Control	CPF 50 μg/L	-6.863	0.271	-19.411	5.686
		CPF 100 μg/L	-1.506	0.807	-14.055	11.042
		CPF 150 μg/L	-24.506	0.000*	-37.055	-11.958
		CPF 200 μg/L	-22.122	0.001*	-34.670	-9.573
Mn	Control	CPF 50 μg/L	125.105	0.018*	23.257	226.953
		CPF 100 μg/L	123.385	0.020*	21.538	225.233
		CPF 150 μg/L	57.817	0.253	-44.030	159.665
		CPF 200 μg/L	54.414	0.282	-47.434	156.261

(* indicates $p<0.05$; n=6).

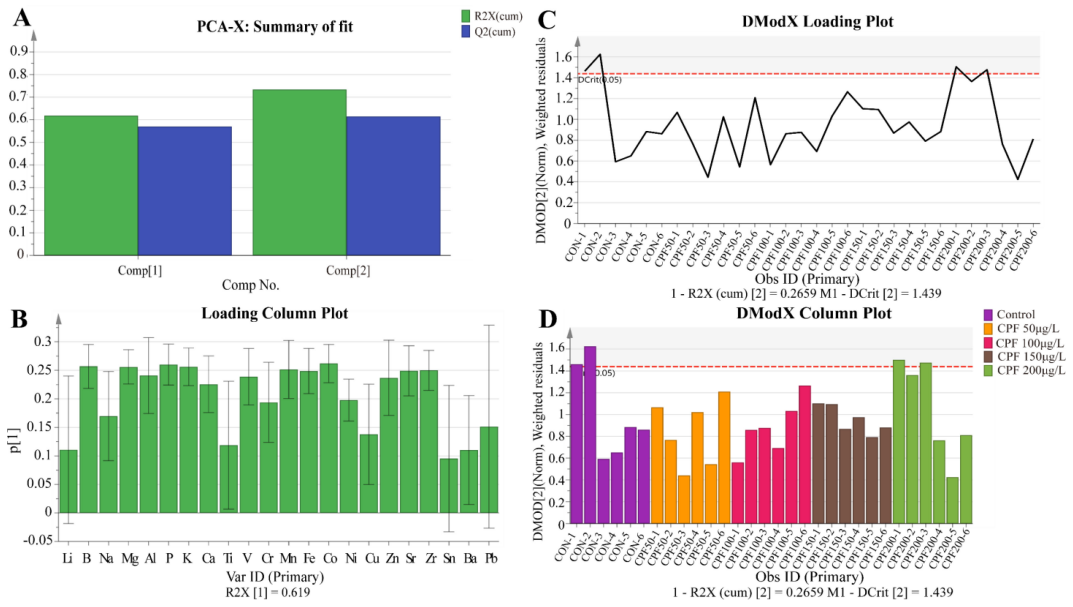

FIGURE 4
PCA of ionomics for Control, CPF 50μg/L, CPF 100μg/L, CPF 150μg/L, and CPF 200μg/L treatments. **(A)** The principal components of the PCA model. **(B)** DModX values of the PCA model. **(C)** Ion parameters contributing to DModX. **(D)** DModX values for each sample. (n=6).

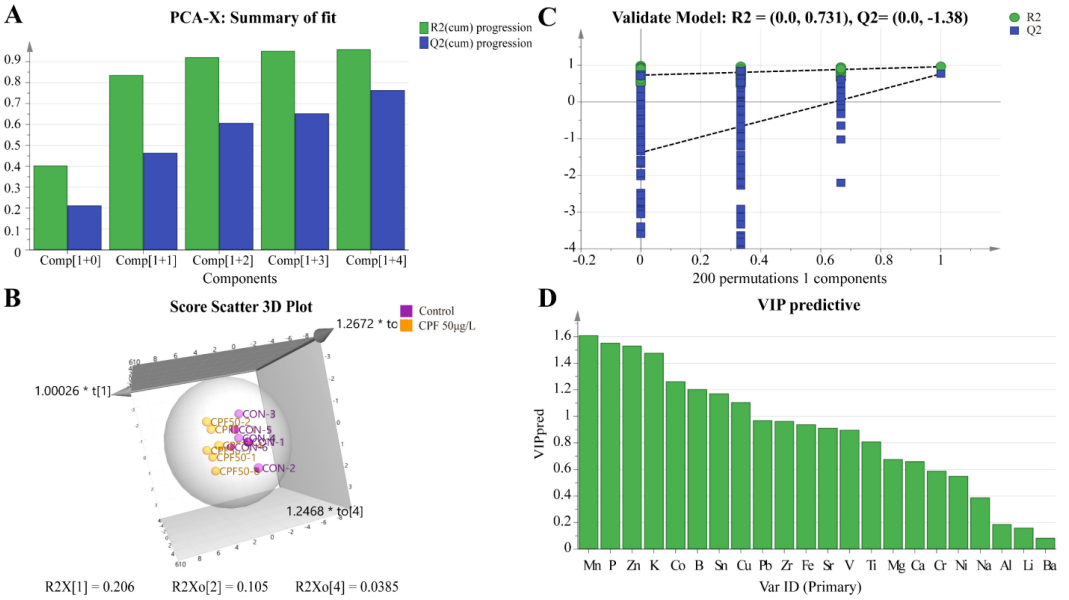

FIGURE 5
OPLS-DA of ionomics between Control and CPF 50 μg/L groups. **(A)** Score plot of the OPLS-DA model. **(B)** Results of 200 permutation tests validating the OPLS-DA model. **(C)** The 3D score scatter plot of OPLS-DA. **(D)** The VIP values for ions in the OPLS-DA model. (n=6).

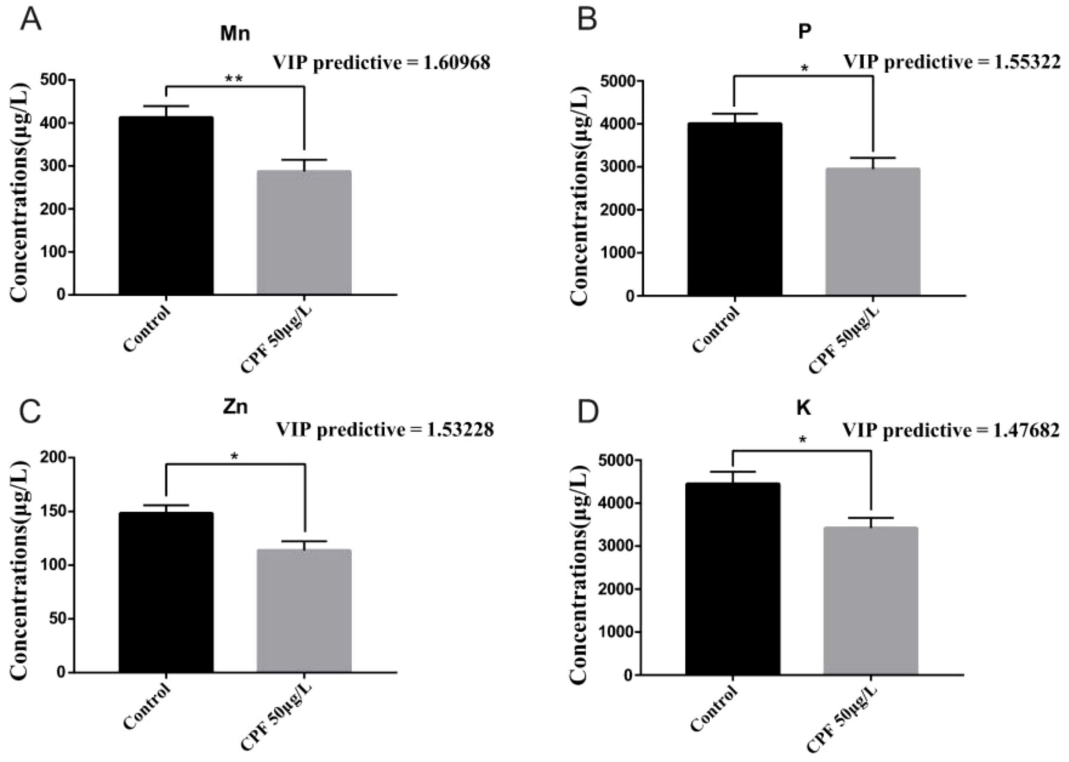

FIGURE 6
OPLS-DA (VIP> 1) and Student's *t*-test analysis of Mn **(A)**, P **(B)**, Zn **(C)** and K **(D)** between Control group and the CPF 50 μg/L group(* $p < 0.05$; ** $p<0.01$; n=6).

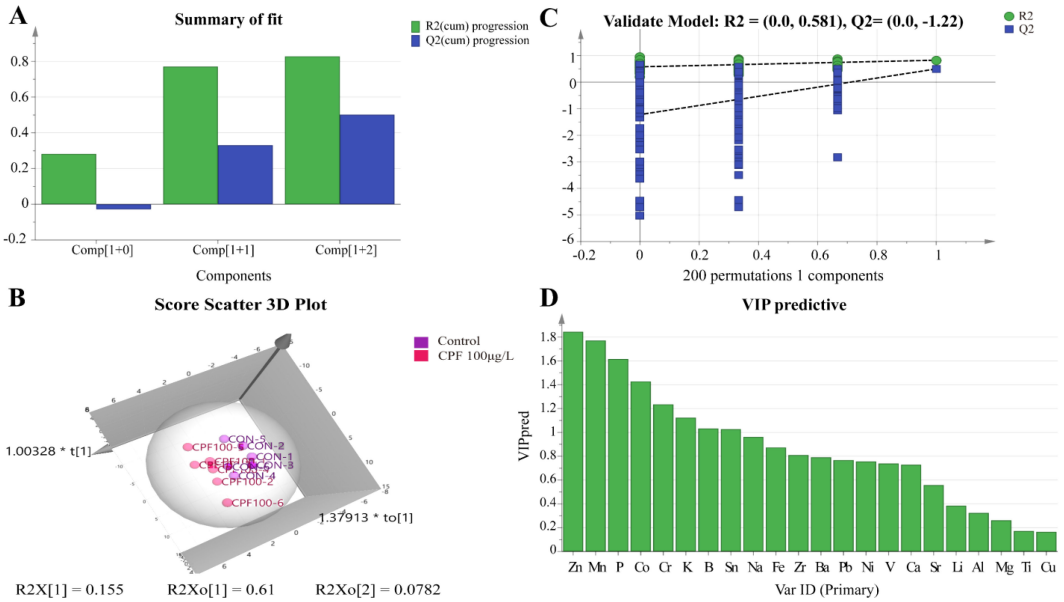

FIGURE 7
OPLS-DA analysis of ionomics between Control and CPF 100 μg/L. **(A)** Score plot of the OPLS-DA model. **(B)** Results of 200 permutation tests for the OPLS-DA. **(C)** The 3D score scatter plot of OPLS-DA model. **(D)** The VIP values of ions from OPLS-DA model. (n=6).

involved in insecticidal action (Dupraz et al., 2019). But the certain concentrations of CPF can also impact physiological characteristics of marine phytoplankton by potentially altering cell membrane permeability in marine microalgae, affecting photosynthetic activity, and increasing reactive oxygen species leading to oxidative stress that affects their growth (DeLorenzo and Serrano, 2003; Tato and Beiras, 2019). We investigated the impact of 200 μg/L CPF on the growth of *Chlorella vulgaris* and found significant inhibition. Similar toxic responses were observed in *Dunaliella tertiolecta* exposed to 600 μg/L CPF (DeLorenzo and Serrano, 2003). The EC50 values for inhibition of growth by CPF were determined as 132 μg/L for *Isochrysis galbana* and 746 μg/L for *Phaeodactylum tricornutum* (Tato and Beiras, 2019). It appears that there is a critical concentration of CPF beyond which significant changes occur in the biological behavior of microalgae.

Generally, trace elements and heavy metal elements primarily affect algae in terms of their growth metabolism rate, photosynthesis, changes in cell size and morphology, as well as enzyme activity (Jin-fen et al., 2000). Mn is a necessary element for physiological and biochemical reactions in microalgae and often serves as an important factor inducing red tide. Photosynthesis has an absolute demand for Mn, because it can exist in four oxidation states, allowing sequential electron transfer from photosystem II-water oxidizing system (Andresen et al., 2018; Kaur et al., 2023). Besides, Mn plays an important role in diverse processes (e.g. chloroplast development, phospholipid biosynthesis, ROS scavenging, respiration and hormone signaling (Hashimoto et al., 2012)) and is required as a cofactor in many enzymes such as decarboxylases and dehydrogenases (Kaur et al., 2023). Zn is an important component of various dehydrogenases and proteases within cellular bodies. Some enzymes are highly sensitive to Zn deficiency, exhibiting strong specificity during metabolic processes. Studies have found that *Eugiena graci* is cytoplasmic nucleoids contain abundant zinc; when experiencing zinc deficiency, these organelles become unstable (Prask and Plocke, 1971). It is generally believed that K can stimulate and control the production of acidic

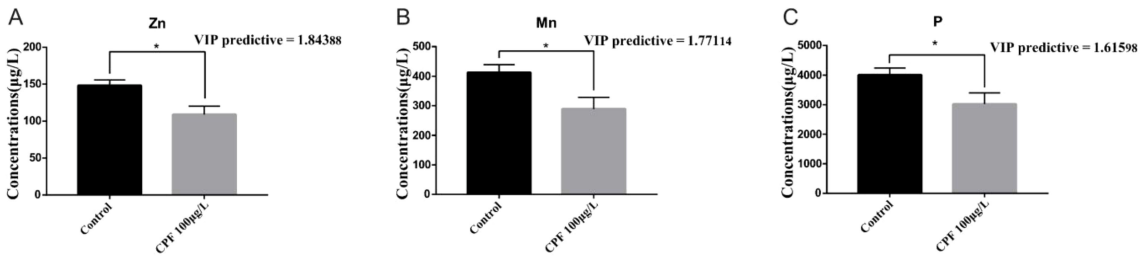

FIGURE 8
OPLS-DA (VIP > 1) and Student's *t*-test analysis of Zn **(A)**, Mn **(B)** and P **(C)** between Control and CPF 100 μg/L groups(* $p < 0.05$; n=6).

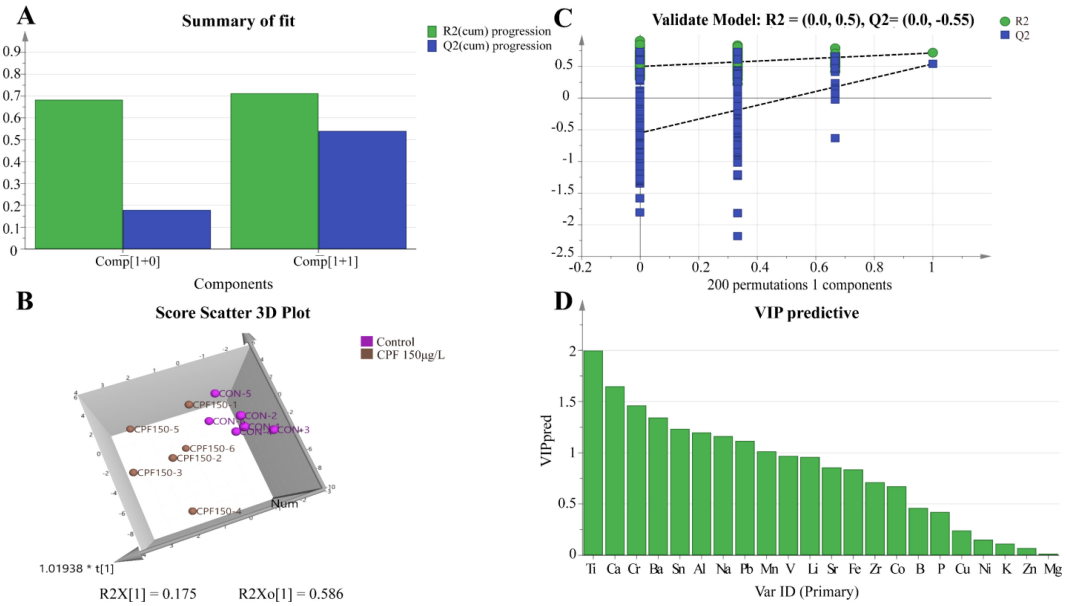

FIGURE 9
OPLS-DA analysis of ionomics between Control and CPF 150 μg/L groups. **(A)** OPLS-DA score plot. **(B)** Results of 200 permutation tests for OPLS-DA model validation. **(C)** The 3D scatter plot of OPLS-DA scores. **(D)** The VIP values for ions in the OPLS-DA model. (n=6).

stimulation by ATPase on the plasma membrane, leading to cell wall relaxation and hydrolase activation, thereby promoting cell growth (Oosterhuis et al., 2014; Ameen et al., 2024). Besides, K performs a critical function in regulating the osmotic pressure, facilitating the transport of photosynthates, sustaining ion homeostasis and activating enzymes. In addition, P is also a common element required for the growth of microalgae. The content of P in natural seawater is small, but a certain concentration of P is an essential nutrient for the growth of microalgae (Biao and Kaijin, 2007). We observed a reduction in the aforementioned elements in the lower dose groups (50 μg/L and 100 μg/L), which may explain why CPF inhibits their growth. Interestingly, no changes were observed in these ions when CPF concentration was increased to 150 μg/L and 200 μg/L; instead, there was an increase in Ti, Li, and Ca ion levels.

External abiotic stresses can disrupt intracellular ion homeostasis. Under salty stress, activation of potassium channels by reactive oxygen species (ROS) will low the cytosolic K pool (Ameen et al., 2024). The photosynthetic activity was shown to induce increases in oxygen concentrations and pH of the colonial cells, and those increases were suggested to favor the precipitation and accumulation of Mn (Schoemann et al., 2001). The exist of function groups like amine, hydroxyl, carboxyl, and phosphoryl group (-NH_2, -OH, -COO and -PO_3^{2-}, respectively) makes the cell surface of microalgae constitute a negative charge, which facilitates the attachment of toxic compounds with positive charge and allows

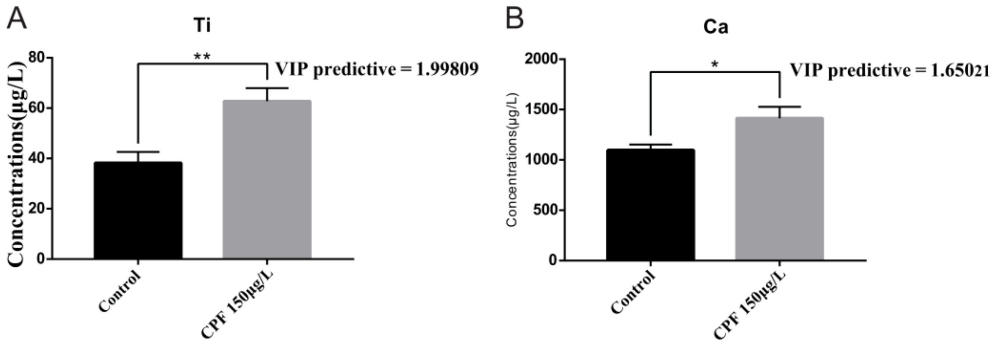

FIGURE 10
Comparison of elemental concentrations, including Ti **(A)** and Ca **(B)**, between the Control group and the CPF 150 μg/L group using OPLS-DA (VIP > 1) and Student's *t*-test (* $p < 0.05$; ** $p<0.01$; n=6).

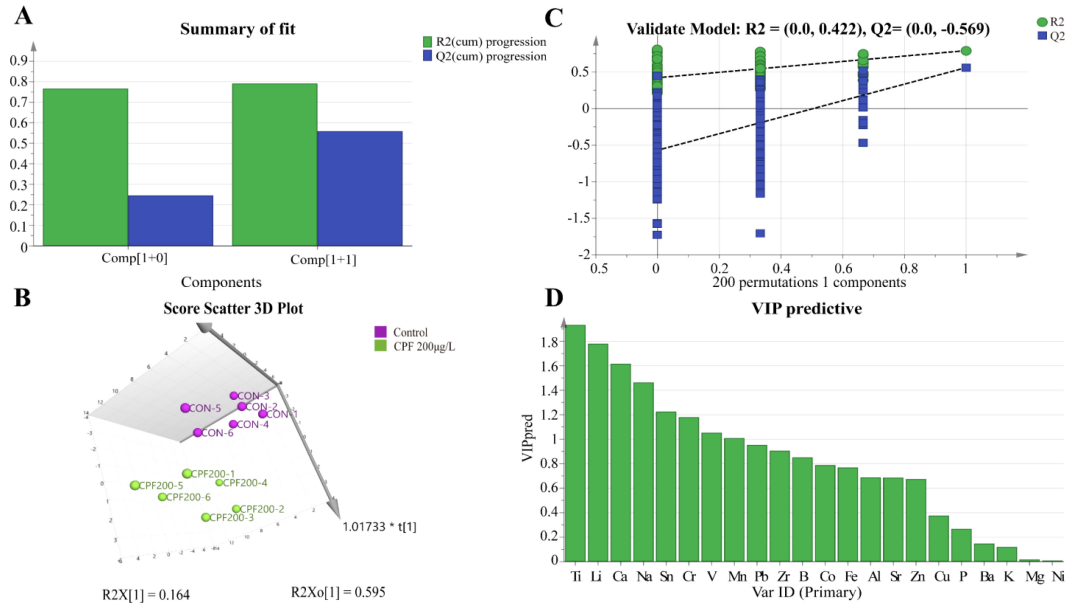

FIGURE 11
OPLS-DA analysis of ionomics between Control and CPF 200 μg/L groups. **(A)** OPLS-DA score plot. **(B)** Results of 200 permutation tests for OPLS-DA model validation. **(C)** The 3D score scatter plot of OPLS-DA. **(D)** The VIP plot for ions in OPLS-DA. (n=6).

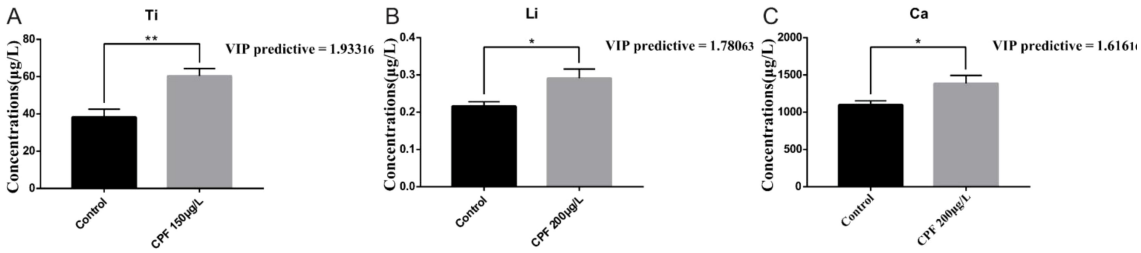

FIGURE 12
Comparison of elemental concentrations, including Ti **(A)**, Li **(B)**, and Ca **(C)**, between the Control group and the CPF 200 μg/L group using OPLS-DA (VIP > 1) and Student's t-test (* $p < 0.05$; ** $p < 0.01$; n = 6).

their sorption (Fayaz et al., 2024). Previous studies have shown that exposure to CPF can harm the cellular membranes and photosystem of microalgae and led to a significant rise in ROS (Baruah et al., 2024). Reasons led to the changes in ion levels of *Chlorella vulgaris* in this study may include the following: (1) CPF destroys the cell membrane structure, resulting in restricted ion transport; (2) CPF binds to the functional groups on the cell surface and saturates the binding sites, which is not conducive to the adsorption of ions by microalgae; (3) CPF exposure damages the photosynthesis system of microalgae, affecting the accumulation of ions (4) CPF stress causes an increase in ROS, resulting in a decrease in ion levels.

When exposed to different concentrations of CPF, the changes in the ion levels of *Chlorella* are different. Changes in individual ion levels or ratios of multiple ions in microalgae may be used as a biomarker to identification the degree of CPF contamination. Compared with other biomarkers (SOD, pigments of microalgae (Shao et al., 2016), etc.), ionomic analysis is more convenient and quick, and this deserves further exploration and verification.

5 Conclusions

The present study not only elucidates the direct impact of CPF on green algae growth but also uncovers potential toxic mechanisms through ionomic analysis, indicating that CPF may impede their growth by disrupting the homeostasis of crucial elements within algal cells. This finding is pivotal for comprehending the potential threat posed by CPF to marine ecosystems and devising effective environmental protection strategies and provides a valuable insights and directions for further research into the mechanism of action of CPF on microalgae. Subsequent investigations should further explore the effects of CPF on other aquatic organisms and entire ecosystems, as well as seek efficient pollution mitigation measures.

Data availability statement

The original contributions presented in the study are included in the article/Supplementary Material. Further inquiries can be directed to the corresponding author/s.

Author contributions

QY: Investigation, Writing – original draft, Writing – review & editing, Data curation, Formal analysis, Resources. YZ: Data curation, Investigation, Writing – original draft, Writing – review & editing. SZ: Data curation, Funding acquisition, Investigation, Resources, Writing – original draft. MP: Formal analysis, Funding acquisition, Methodology, Resources, Supervision, Writing – original draft, Writing – review & editing. PJ: Data curation, Formal analysis, Investigation, Supervision, Writing – original draft. PQ: Conceptualization, Methodology, Project administration, Supervision, Writing – review & editing.

Funding

The author(s) declare financial support was received for the research, authorship, and/or publication of this article.

Acknowledgments

This work was financially supported by Laoshan Laboratory (Grant No. LSKJ202203902), the Natural Science Foundation of Shandong Province, China (Grant No. ZR2021MD014 and ZR2022MD027), and Key R&D Program of Jining (Grant No. 2022YXNS121).

Conflict of interest

The authors declare that the research was conducted in the absence of any commercial or financial relationships that could be construed as a potential conflict of interest.

Generative AI statement

The author(s) declare that no Generative AI was used in the creation of this manuscript.

Publisher's note

All claims expressed in this article are solely those of the authors and do not necessarily represent those of their affiliated organizations, or those of the publisher, the editors and the reviewers. Any product that may be evaluated in this article, or claim that may be made by its manufacturer, is not guaranteed or endorsed by the publisher.

Supplementary material

The Supplementary Material for this article can be found online at: https://www.frontiersin.org/articles/10.3389/fmars.2025.1524885/full#supplementary-material

References

Affum, A. O., Acquaah, S. O., Osae, S. D., and Kwaansa-Ansah, E. E. (2018). Distribution and risk assessment of banned and other current-use pesticides in surface and groundwaters consumed in an agricultural catchment dominated by cocoa crops in the Ankobra Basin, Ghana. *Sci. Total Environ.* 633, 630–640. doi: 10.1016/j.scitotenv.2018.03.129

Ameen, M., Akhtar, J., Anwar-ul-Haq, M., Abbasi, G. H., Ali, M., Ali, Q., et al. (2024). "Potassium in plants: possible functions, mechanisms and proteomics under abiotic environmental stress," in *Metals and Metalloids in Plant Signaling*. Ed. T. Aftab (Cham, Switzerland: Springer), 73–110. doi: 10.1007/978-3-031-59024-5_5

Andresen, E., Peiter, E., and Küpper, H. (2018). Trace metal metabolism in plants. *J. Exp. Bot.* 69, 909–954. doi: 10.1093/jxb/erx465

Balmer, J. E., Morris, A. D., Hung, H., Jantunen, L., Vorkamp, K., Rigét, F., et al. (2019). Levels and trends of current-use pesticides (CUPs) in the arctic: An updated review, 2010–2018. *Emerging Contaminants* 5, 70–88. doi: 10.1016/j.emcon.2019.02.002

Baruah, P., Srivastava, A., Mishra, Y., and Chaurasia, N. (2024). Modulation in growth, oxidative stress, photosynthesis, and morphology reveals higher toxicity of alpha-cypermethrin than chlorpyrifos towards a non-target green alga at high doses. *Environ. Toxicol. Pharmacol.* 106, 104376. doi: 10.1016/j.etap.2024.104376

Bellas, J., García-Pimentel-M-d, M., and León, V. M. (2023). "Chapter 7 - Current-use pesticides in the marine environment," in *Contaminants of emerging concern in the marine environment*. Eds. V. M. León and J. Bellas (Amsterdam, Netherlands: Elsevier), 229–309. doi: 10.1016/B978-0-323-90297-7.00010-X

Biao, X., and Kaijin, Y. (2007). Shrimp farming in China: Operating characteristics, environmental impact and perspectives. *Ocean Coast. Manage.* 50, 538–550. doi: 10.1016/j.ocecoaman.2007.02.006

DeLorenzo, M., and Serrano, L. (2003). Individual and mixture toxicity of three pesticides; atrazine, chlorpyrifos, and chlorothalonil to the marine phytoplankton species *Dunaliella tertiolecta*. *J. Environ. Sci. Health Part B Pesticides Food contaminants Agric. wastes* 38, 529–538. doi: 10.1081/PFC-120023511

Dupraz, V., Stachowski-Haberkorn, S., Wicquart, J., Tapie, N., Budzinski, H., and Akcha, F. (2019). Demonstrating the need for chemical exposure characterisation in a microplate test system: toxicity screening of sixteen pesticides on two marine microalgae. *Chemosphere* 221, 278–291. doi: 10.1016/j.chemosphere.2019.01.035

EPA (1986).Pesticide ecotoxicity database of the office of pesticide programs, ecological fate and effects division. Available online at: https://www.epa.gov/endangered-species/biological-evaluation-chapters-chlorpyrifos-esa-assessment (Accessed January 3, 2025).

FAO (2024).The State of World Fisheries and Aquaculture 2024 – Blue Transformation in action. Available online at: https://openknowledge.fao.org/handle/20.500.14283/cd0683en (Accessed January 3, 2025).

Fayaz, T., Rana, S. S., Goyal, E., Ratha, S. K., and Renuka, N. (2024). Harnessing the potential of microalgae-based systems for mitigating pesticide pollution and its impact on their metabolism. *J. Environ. Manage.* 357, 120723. doi: 10.1016/j.jenvman.2024.120723

Guillard, R. R. L. (1975). "Culture of phytoplankton for feeding marine invertebrates," in *Culture of Marine Invertebrate Animals: Proceedings — 1st Conference on Culture of Marine Invertebrate Animals Greenport*. Eds. W. L. Smith and M. H. Chanley (Boston, MA: Springer), 29–60. doi: 10.1007/978-1-4615-8714-9_3

Hashimoto, K., Eckert, C., Anschütz, U., Scholz, M., Held, K., Waadt, R., et al. (2012). Phosphorylation of calcineurin B-like (CBL) calcium sensor proteins by their CBL-interacting protein kinases (CIPKs) is required for full activity of CBL-CIPK complexes

toward their target proteins*. *J. Biol. Chem.* 287, 7956–7968. doi: 10.1074/jbc.M111.279331

Huang, X., Cui, H., and Duan, W. (2020). Ecotoxicity of chlorpyrifos to aquatic organisms: A review. *Ecotoxicology Environ. Saf.* 200, 110731. doi: 10.1016/j.ecoenv.2020.110731

Jiang, Y., He, Y., Li, W., Ni, J., Li, J., Peng, L., et al. (2021). Exposure to chlorpyrifos leads to spindle disorganization and mitochondrial dysfunction of porcine oocytes during *in vitro* maturation. *Theriogenology* 173, 249–260. doi: 10.1016/j.theriogenology.2021.08.007

Jin-fen, P., Rong-gen, L., and Li, M. (2000). A review of heavy metal adsorption by marine algae. *Chin. J. Oceanology Limnology* 18, 260–264. doi: 10.1007/BF02842673

Kar, A., Deole, S., Nayak, R. R., Gupta, A. K., Gadratagi, B. G., Patil, N., et al. (2024). Distribution and risk assessment of pesticide pollution in small streams adjoining paddy fields. *J. Hazardous Materials* 469, 133852. doi: 10.1016/j.jhazmat.2024.133852

Kaur, H., Kaur, H., Kaur, H., and Srivastava, S. (2023). The beneficial roles of trace and ultratrace elements in plants. *Plant Growth Regul.* 100, 219–236. doi: 10.1007/s10725-022-00837-6

Key, P. B., and Fulton, M. H. (1993). Lethal and sublethal effects of chlorpyrifos exposure on adult and larval stages of the grass shrimp, *Palaemonetes pugio*. *J. Environ. Sci. Health Part B* 28, 621–640. doi: 10.1080/03601239309372844

Li, Q., Zhu, K., Liu, L., and Sun, X. (2021). Pollution-induced food safety problem in China: trends and policies. *Front. Nutr.* 8. doi: 10.3389/fnut.2021.703832

Liu, L., Tang, J., Zhong, G., Zhen, X., Pan, X., and Tian, C. (2018). Spatial distribution and seasonal variation of four current-use pesticides (CUPs) in air and surface water of the Bohai Sea, China. *Sci. Total Environ.* 621, 516–523. doi: 10.1016/j.scitotenv.2017.11.282

Montuori, P., Aurino, S., Nardone, A., Cirillo, T., and Triassi, M. (2015). Spatial distribution and partitioning of organophosphates pesticide in water and sediment from Sarno River and Estuary, Southern Italy. *Environ. Sci. pollut. Res.* 22, 8629–8642. doi: 10.1007/s11356-014-4016-z

Morris, A. D., Muir, D. C. G., Solomon, K. R., Letcher, R. J., McKinney, M. A., Fisk, A. T., et al. (2016). Current-use pesticides in seawater and their bioaccumulation in polar bear–ringed seal food chains of the Canadian Arctic. *Environ. Toxicol. Chem.* 35, 1695–1707. doi: 10.1002/etc.3427

Nandi, N. K., Vyas, A., Akhtar, M. J., and Kumar, B. (2022). The growing concern of chlorpyrifos exposures on human and environmental health. *Pesticide Biochem. Physiol.* 185, 105138. doi: 10.1016/j.pestbp.2022.105138

Oosterhuis, D. M., Loka, D. A., Kawakami, E. M., and Pettigrew, W. T. (2014). "Chapter three - the physiology of potassium in crop production," in *Advances in Agronomy*. Ed. D. L. Sparks (Cambridge, US: Academic Press), 203–233. doi: 10.1016/B978-0-12-800132-5.00003-1

Prask, J. A., and Plocke, D. J. (1971). A role for zinc in the structural integrity of the cytoplasmic ribosomes of Euglena gacilis. *Plant Physiol.* 48, 150–155. doi: 10.1104/pp.48.2.150

Rao, J. V., Rani, C. H. S., Kavitha, P., Rao, R. N., and Madhavendra, S. S. (2003). Toxicity of chlorpyrifos to the fish *Oreochromis mossambicus*. *Bull. Environ. Contamination Toxicol.* 70, 0985–0992. doi: 10.1007/s00128-003-0079-0

Roast, S. D., Thompson, R. S., Donkin, P., Widdows, J., and Jones, M. B. (1999). Toxicity of the organophosphate pesticides chlorpyrifos and dimethoate to *Neomysis integer* (Crustacea: Mysidacea). *Water Res.* 33, 319–326. doi: 10.1016/S0043-1354(98)00248-6

Ros, O., Izaguirre, J. K., Olivares, M., Bizarro, C., Ortiz-Zarragoitia, M., Cajaraville, M. P., et al. (2015). Determination of endocrine disrupting compounds and their metabolites in fish bile. *Sci. Total Environ.* 536, 261–267. doi: 10.1016/j.scitotenv.2015.07.074

Schoemann, V., Wollast, R., Chou, L., and Lancelot, C. (2001). Effects of photosynthesis on the accumulation of Mn and Fe by Phaeocystis colonies. *Limnol. Oceanogr.* 46, 1065–1076. doi: 10.4319/lo.2001.46.5.1065

Shao, Y., Li, Y., Jiang, L., Pan, J., He, Y., and Dou, X. (2016). Identification of pesticide varieties by detecting characteristics of *Chlorella pyrenoidosa* using Visible/Near infrared hyperspectral imaging and Raman microspectroscopy technology. *Water Res.* 104, 432–440. doi: 10.1016/j.watres.2016.08.042

Singh, A., Jaiswal, A., Singh, A., Tomar, R. S., and Kumar, A. (2022). "Chapter 9 - Plant ionomics: toward high-throughput nutrient profiling," in *Suprasanna P. Plant Nutrition and Food Security in the Era of Climate Change*. Eds. V. Kumar and A. K. Srivastava (Cambridge, US: Academic Press), 227–254. doi: 10.1016/B978-0-12-822916-3.00015-9

Smalling, K. L., Kuivila, K. M., Orlando, J. L., Phillips, B. M., Anderson, B. S., Siegler, K., et al. (2013). Environmental fate of fungicides and other current-use pesticides in a central California estuary. *Mar. pollut. Bull.* 73, 144–153. doi: 10.1016/j.marpolbul.2013.05.028

Solé, M., Porte, C., Barcelo, D., and Albaiges, J. (2000). Bivalves residue analysis for the assessment of coastal pollution in the Ebro Delta (NW Mediterranean). *Mar. pollut. Bull.* 40, 746–753. doi: 10.1016/S0025-326X(00)00011-4

Sun, K., Wang, N., Liu, L. L., and Duan, S. S. (2013). Ecological risks assessment of organophosphorus pesticides based on response of Scenedesmus quadricanda. *China Environ. Sci.* 33, 868–873. doi: 10.0000/j.zghjkx.1000-6923.20133313250

Tato, T., and Beiras, R. (2019). The use of the marine microalga *Tisochrysis lutea* (T-iso) in standard toxicity tests; Comparative sensitivity with other test species. *Front. Mar. Sci.* 6. doi: 10.3389/fmars.2019.00488

Ubaid ur Rahman, H., Asghar, W., Nazir, W., Sandhu, M. A., Ahmed, A., and Khalid, N. (2021). A comprehensive review on chlorpyrifos toxicity with special reference to endocrine disruption: Evidence of mechanisms, exposures and mitigation strategies. *Sci. Total Environ.* 755, 142649. doi: 10.1016/j.scitotenv.2020.142649

Walsh, G. E., McLaughlin, L. L., Yoder, M. J., Moody, P. H., Lores, E. M., Forester, J., et al. (1988). *Minutocellus polymorphus*: A new marine diatom for use in algal toxicity tests. *Environ. Toxicol. Chem.* 7, 925–929. doi: 10.1002/etc.5620071109

Zargar, S. M., Gupta, N., Nazir, M., Mir, R. A., Gupta, S. K., Agrawal, G. K., et al. (2016). "Chapter 13 - omics – A new approach to sustainable production," in *Breeding Oilseed Crops for Sustainable Production*. Ed. S. K. Gupta (Cambridge, US: Academic Press), 317–344. doi: 10.1016/B978-0-12-801309-0.00013-6

Zhao, Y. Q., Li, L. N., and Li, J. H. (2008). Study of acute and joint toxicity of common pyrethroid and organophosphate pesticides to fish. *Environ. pollut. Control* 11, 53–57. doi: 10.3969/j.issn.1001-3865.2008.11.013

Zhong, G., Xie, Z., Cai, M., Möller, A., Sturm, R., Tang, J., et al. (2012). Distribution and air–sea exchange of current-use pesticides (CUPs) from East Asia to the High Arctic Ocean. *Environ. Sci. Technol.* 46, 259–267. doi: 10.1021/es202655k

Zhou, S., Duan, C., Wang, X., Michelle, W. H. G., Yu, Z., and Fu, H. (2008). Assessing cypermethrin-contaminated soil with three different earthworm test methods. *J. Environ. Sci.* 20, 1381–1385. doi: 10.1016/S1001-0742(08)62236-6